Materials Letters 282 (2021) 128677

Contents lists available at ScienceDirect

Materials Letters

journal homepage: www.elsevier.com/locate/mlblue

Orientation dependence of superelasticity in quenched high-nickel Ti-51.8Ni single crystals

E.E. Timofeeva [a,*], E.Yu. Panchenko [a], A.I. Tagiltsev [a], N.G. Larchenkova [a], A.B. Tokhmetova [a], Yu.I. Chumlyakov [a], M.N. Volochaev [b]

[a] Tomsk State University, Novosobornaya Square 1, Tomsk 634050, Russia
[b] Kirensky Institute of Physics, FRC KSC SB RAS, Krasnoyarsk 660036, Russia

ARTICLE INFO

Article history:
Received 23 June 2020
Accepted 11 September 2020
Available online 16 September 2020

Keywords:
Phase transformation
Shape memory materials
Ti-Ni
Single crystals
Superelasticity
Strain-glass

ABSTRACT

The orientation dependence of the functional and mechanical properties of quenched Ti-51.8at.%Ni single crystals, undergoing a strain-glass transition upon cooling/heating was investigated. It was found that a compressive stress above 800 MPa leads to the B2-B19′ martensitic transformation (MT), regardless of orientation. In the high-strength [001]-orientation, superelasticity (SE) was observed at 203–248 K, with a reversible strain of 2.3%. Degradation of SE at deforming stresses σ > 1000 MPa was associated with the formation of $\{113\}_{B2}$ twins during the reverse MT. In the low-strength $[1\ 1\ \bar{1}]$-orientation, the formation of stress-induced B19′-martensite occurred simultaneously with the plastic deformation of the B2-phase (due to the formation of reorientation bands and dislocation slip) and a reversible strain was not observed.

1. Introduction

Thermoelastic B2-B19′ MTs are not observed upon cooling in the high-nickel quenched TiNi alloys with C_{Ni} > 51.2at.% [1,2]. The B2-matrix contains numerous point defects (substitutional defects, excess Ni atoms in the Ti sublattice), which form the local deformations, disturb the long-range order and prevent the appearance of martensite lamellae. In this case, a transition from unfrozen strain-glass into frozen strain-glass occurs during stress-free cooling down to T_g temperature [1,2]. Despite the absence of thermal-induced MT, the stress-induced B2-B19′ MTs are possible in these alloys, and therefore, shape memory effect (SME) and SE. In Refs. [3,4] the temperature dependences of stress hysteresis and critical stresses along the SE temperature range were investigated on strain-glass TiNi polycrystals. However, the influence of orientation on stress-induced B2-B19′ MT in strain-glass TiNi single crystals is poorly studied. The authors know of only one work dedicated to the orientation dependence of SE in high-nickel TiNi crystals with C_{Ni} > 51.2at.% [5]. It focuses on the SE in aged single crystals, in which the Ni content of the matrix is C_{Ni} < 51.2at.% and thermal-induced MT is observed. Therefore, the aim of the work is to investigate the stress-induced B2-B19′ MT under compression in quenched Ti-51.8at.%Ni single crystals, depending on the orientation and test temperature.

2. Materials and methods

Ti-51.8at.%Ni single crystals were grown by the Bridgman method. Samples for compression had a parallelepiped shape with sizes of $(3 \times 3 \times 6)\mathrm{mm}^3$. The strain-glass transformation was investigated by a DMA/SDTA861 dynamic mechanical analyser (preload 15 N, speed 2 K/min, tension, maximum strain 10 μm) and by measuring the temperature dependence of the electrical resistance. Mechanical tests were carried out on Instron VHS 5969. Two orientations were chosen for the study:

1) [001]-orientation, in which the Schmid factor for a ⟨100⟩{011} and a ⟨001⟩{001} slip systems in the B2-phase is equal to zero, |m|=0, and slip is suppressed [5], and so the deformation of the B2-phase develops by twinning at high stresses [6]. For [001]-oriented crystals in compression, no detwinning of B19′-martensite is observed ($\varepsilon_{CVP} = \varepsilon_{CVP+detw}$ = 4.4% [7]);

2) $[1\ 1\ \bar{1}]$-orientation, in which the Schmid factor |m|=0.47 for a ⟨100⟩{011} [5] and the detwinning of B19′-martensite under applied stress is observed (ε_{CVP} = 3.5%, $\varepsilon_{CVP+detw}$ = 3.8% [7]). Single crystals were preliminarily annealed at 1253 K for 1 h, followed by water quenching. Electron microscopy studies were carried out on a Philips CM-12 and HT-7700 Hitachi.

* Corresponding author.
E-mail address: katie@sibmail.com (E.E. Timofeeva).

https://doi.org/10.1016/j.matlet.2020.128677
0167-577X/

3. Results and discussion

It was experimentally established that, upon cooling, thermal-induced MTs were not observed in quenched Ti-51.8at.%Ni single crystals (Fig. 1, a). Instead, a strain-glass transition occurs (Fig. 1, b). The true temperature of strain-glass transition T_0 was determined, as the temperature of the internal friction peak Tg at $\omega \to 0$ Hz: T_0 = 155 K is consistent with [1].

Fig. 2 shows the results of mechanical tests in loading/unloading cycles at different temperatures $T \geq T_0$. It is possible to observe the SE at 203–248 K with a reversible strain of up to 2.3% during compression along the [001]-orientation (Fig. 2, a). Above the temperature T = 248 K, only partial reversibility was obtained. For $\left[1\ 1\ \bar{1}\right]$-oriented crystals all the given strain was irreversible, even after heating the sample (Fig. 2, b).

The temperature dependences of the critical stresses $\sigma_{cr}(T)$ were plotted using the $\sigma(\varepsilon)$ curves at various temperatures (Fig. 2, c). The level of deforming stresses at 200 K (near T_0) was very high $\sigma_{cr} \approx 800$ MPa and was weakly dependent on orientation. The absence of the orientation dependence of σ_{cr} near the start temperature M_s of thermal-induced MT, was also observed in TiNi alloys [8].

The σ_{cr} values grew with an increase in temperature from T_0 to M_d, which is typical for stress-induced MTs and can be described by the Clapeyron-Clausius equation $d\sigma_{cr}/dT = -\Delta S/\varepsilon_{tr}$ [8]. Based on the theoretical strain values $\varepsilon_{CVP+detw}$, the $\alpha_{111} = d\sigma_{cr}/dT$ should be close or slightly higher than $\alpha_{001} = d\sigma_{cr}/dT$. However, the experimental values of α_{111} = 2.4 MPa/K are two times lower than α_{001} = 4.4 MPa/K (Fig. 2), which was also found in [5] during the comparison of the high-strength (⟨001⟩, ⟨110⟩, ⟨012⟩) and the low-strength (⟨111⟩, ⟨122⟩) orientations. Therefore, the orientation dependence of $\alpha = d\sigma_{cr}/dT$ is determined not only by the transformation strain, but also by the entropy change ΔS. A possible reason for the weak growth of stresses σ_{cr} in the $\left[1\ 1\ \bar{1}\right]$-orientation, is associated with the influence of high stresses on the elastic distortion of the B2-lattice, which in the case of the $\left[1\ 1\ \bar{1}\right]$-orientation has rhombohedral distortions close to monoclinic. As a result, $\Delta S_{111} < \Delta S_{001}$ and $\alpha_{111} < \alpha_{001}$.

The stresses σ_{cr} reached a maximum value at $T = M_d$, and, σ_{cr} decreased at $T > M_d$. For the $\left[1\ 1\ \bar{1}\right]$-orientation M_d = 353 K and $\sigma_{cr}(M_d)$ = 1100 MPa, and for the [001]-orientation M_d = 423 K and $\sigma_{cr}(M_d)$ = 1675 MPa.

The large $\{113\}_{B2}$ twins were observed by electron microscope after compression along the [001]-orientation at $T_0 < T < M_d$ (Fig. 3, a). These twins appear due to the forward and reverse B2-B19′-$B2_{tw}$ MTs [9] and could cause the degradation of SE. It is possible to observe a good SE with a low irreversibility at deforming stresses σ < 1GPa. At σ > 1GPa, the SE was accompanied by significant irreversibility. It is assumed that at σ > 1GPa, the high local stresses are achieved and contribute to the formation of $\{113\}_{B2}$ twins during the reverse MT.

In the [111]-oriented single crystals, the reorientation bands of the B2-matrix with a large number of dislocations (Fig. 3, b), and the regions of residual B19′-martensite, twinned by type I $\{11\bar{1}\}$ and type II {011} (Fig. 3, c-e) were observed by electron microscope after compression at $T_0 < T < M_d$. Therefore, the formation of the B19′-martensite during compression along the $\left[1\ 1\ \bar{1}\right]$-orientation was experimentally confirmed.

Thus, in quenched Ti-51.8at.%Ni crystals, the stress-induced B2-B19′ MT with a reversible strain, can be realized in the high-strength [001]-orientation in which the dislocation slip is suppressed (in the a ⟨100⟩{011} and a ⟨001⟩{001} slip systems [5]) and no detwinning of B19′-martensite is observed [7]. However, it is not possible to stabilize B19′-martensite in the [001]-orientation for the same reasons.

In the low-strength $\left[1\ 1\ \bar{1}\right]$-orientation, the B2-B19′ MT occurred simultaneously with the plastic deformation of the B2-phase, due to the high stresses required for the MT (above 800 MPa), close to the yield strength of the B2-phase (maximum is 1100 MPa). In this case, the dislocation slip [5] and the detwinning of B19′-martensite also occurs [7], which is accompanied by the rotation of the habit plane and the stress relaxation, with the formation of defects. Therefore, in $\left[1\ 1\ \bar{1}\right]$-oriented crystals, no reversibility could be obtained, but it is possible to stabilize the B19′-martensite.

At $T > M_d$ the residual martensite was not observed by the electron microscope, regardless of orientation. No dislocations were found in the high-strength [001]-oriented crystals, and the deformation of the B2-phase was developed by twinning. In the present work the $\{114\}_{B2}$ twins were found after compression along the [001]-orientation at $T > M_d$ (Fig. 4, a), as in Refs. [10,11]. On the contrary, in the low-strength $\left[1\ 1\ \bar{1}\right]$-oriented crystals, only a high dislocation density formed during deformation at $T > M_d$ (Fig. 4, b), similar to [12].

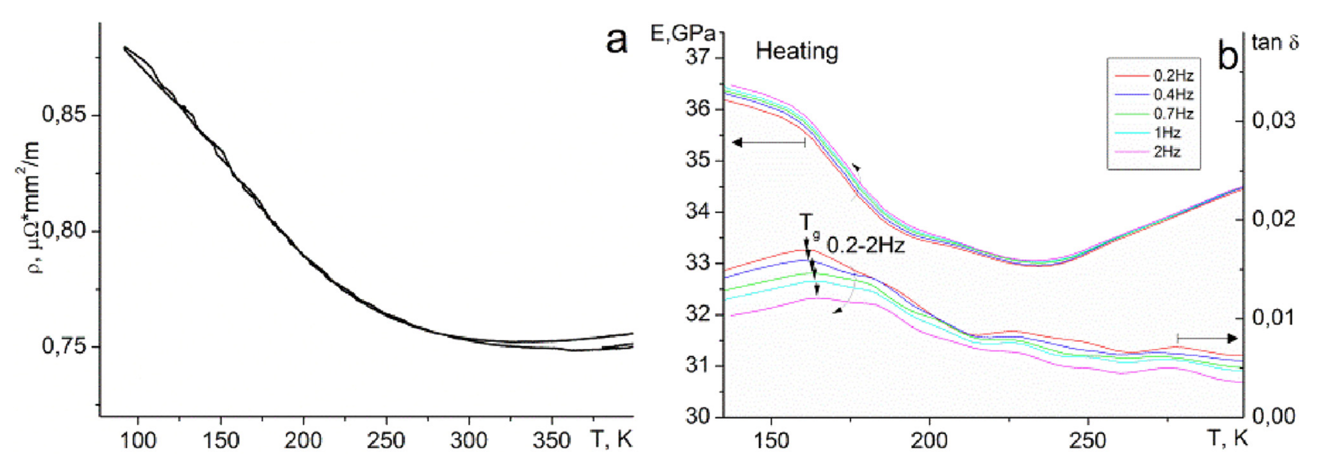

Fig. 1. The temperature dependence of the electrical resistance ρ(T) (a); frequency-temperature dependences of the elastic modulus E and internal friction tan δ (b) for quenched Ti-51.8at.%Ni single crystals.

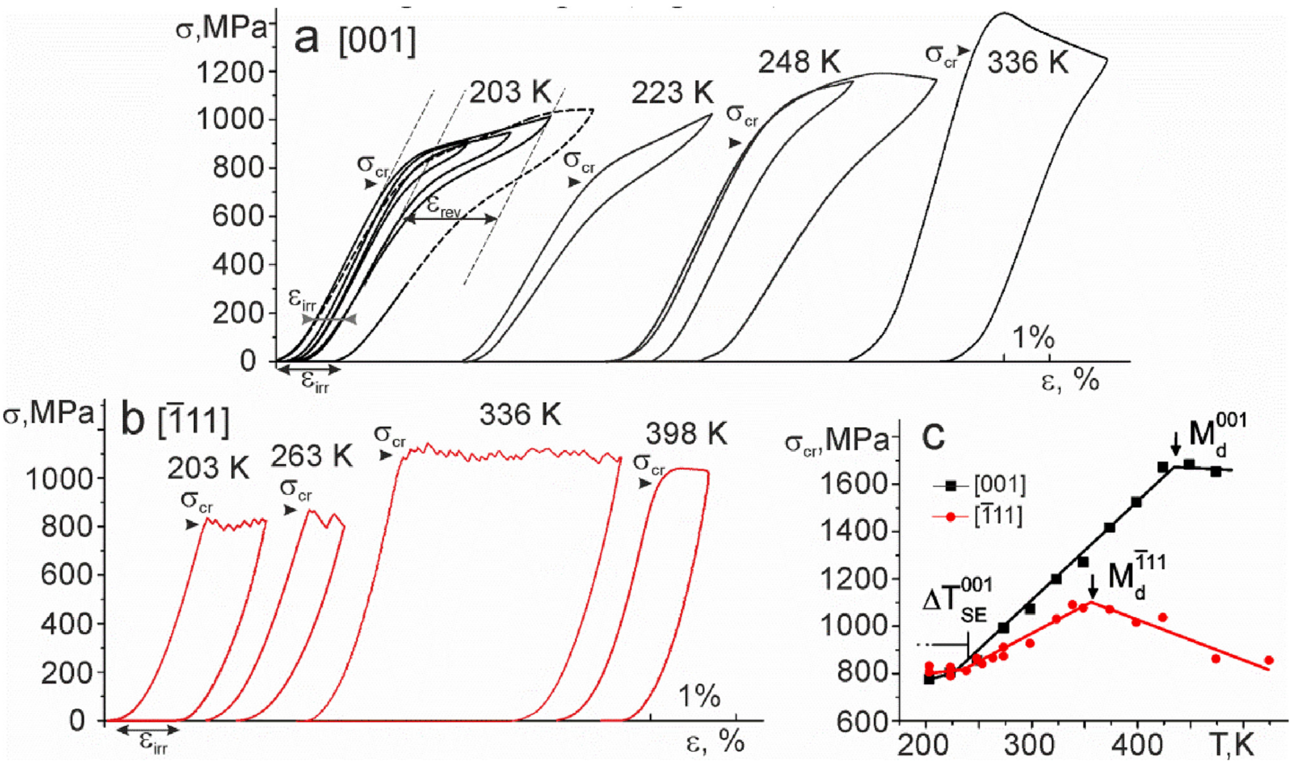

Fig. 2. $\sigma(\varepsilon)$ curves (a, b); temperature dependences of critical stresses $\sigma_{cr}(T)$ (c) in quenched Ti-51.8at.%Ni single crystals.

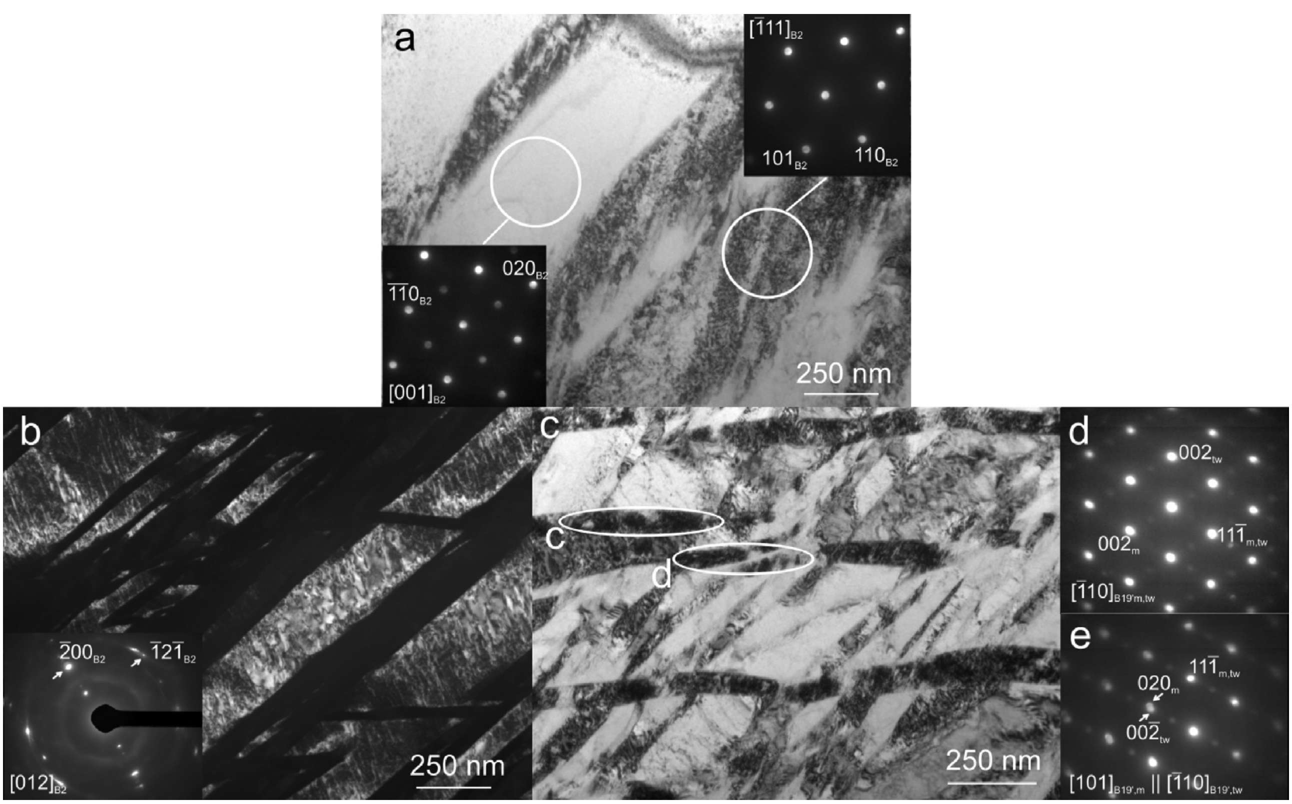

Fig. 3. TEM images of Ti-51.8at.%Ni single crystals after compression at 203 K along the [001]- (a) and [111]-orientations (b-e): bright field and SAEDP, demonstrated twins in the B2-phase, zone axis $[001]_{B2}||\left[1\ 1\ \bar{1}\right]_{B2}$ (a); dark field and SAEDP, demonstrated deformed B2-phase, zone axis $[012]_{B2}$ (b); bright field and SAEDPs, demonstrated residual B19′-martensite (c-e).

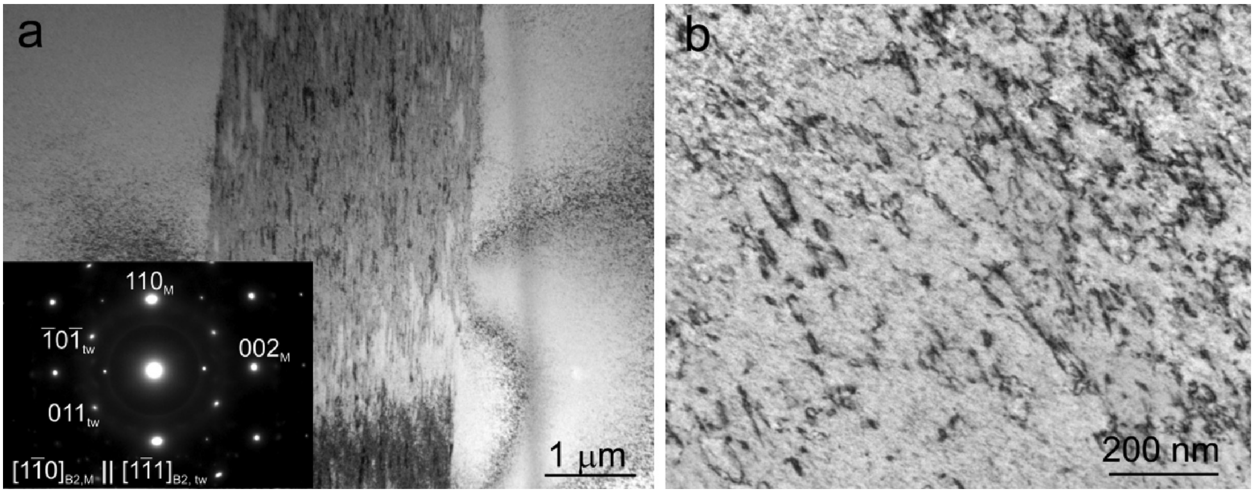

Fig. 4. TEM images of Ti-51.8at.%Ni single crystals after compression at 473 K: [001]-oriented crystals, bright field and SAEDP, zone axis $[10\bar{1}]_{B2,M}||[11\bar{1}]_{B2,tw}$ (a); [111]-oriented crystals, bright field (b).

4. Conclusion

The orientation dependence of the functional and mechanical properties of quenched Ti-51.8at.%Ni single crystals was investigated. The yield strength of the B2-phase reached $\sigma_{cr}(M_d = 423\ K) = 1675$ MPa, and the deformation of the B2-phase at $T > M_d$ occurred by twinning ($\{114\}_{B2}$ twins were observed) in the high-strength [001]-orientation, in which the dislocation slip in a $\langle 100\rangle\{011\}$ and a $\langle 001\rangle\{001\}$ systems is difficult. In the [001]-oriented single crystals, the SE was obtained at 203–248 K with a reversible strain of up to 2.3%, while the applied stresses are less than 1GPa. At $\sigma > 1$GPa the degradation of SE is associated with the formation of $\{113\}_{B2}$ twins during the reverse MT.

In the low-strength $[11\bar{1}]$-orientation, where the dislocation slip easily occurred, the yield strength of the B2-phase was less than in the [001]-orientation, and was equal to $\sigma_{cr}(M_d = 353\ K) = 1100$ MPa. In the $[11\bar{1}]$-orientation, the formation of stress-induced B19′-martensite occurred simultaneously with the plastic deformation of the B2-phase and no reversible strain was observed. The existence of stress-induced B2-B19′ MT was confirmed by electron microscopic observations of residual B19′-martensite.

Declaration of Competing Interest

The authors declare that they have no known competing financial interests or personal relationships that could have appeared to influence the work reported in this paper.

Acknowledgments

This work was supported by the Russian Science Foundation (grant No. 18–19–00298). The electron microscopy studies were carried out on the equipment of the Krasnoyarsk Regional Center for Collective Use SB RAS.

References

[1] Y. Wang, X. Ren, K. Otsuka, Mater. Sci. Forum 583 (2008) 67–84.
[2] X. Ren, Phys. Status Solidi B 251 (2014) 1982–1992.
[3] K. Niitsu, R. Kainuma, Phys. Status Solidi B 251 (2014) 2041–2047.
[4] K. Niitsu, T. Omori, R. Kainuma, Appl. Phys. Lett. 102 (2013) 231915.
[5] H. Sehitoglu, J. Jun, X. Zhang, et al., Acta Mater. 49 (2001) 3609–3620.
[6] N.S. Surikova, O.V. Evtushenko, V.A. Pavlyuk, Phys. Mesomech. 13 (2010) 96–102.
[7] H. Sehitoglu, R. Hamilton, D. Canadinc, et al., Metall. Mater. Trans. A 34A (2003) 5–13.
[8] K. Otsuka, X. Ren, Prog. Mater Sci. 50 (2005) 511–678.
[9] A.N. Tyumentsev, N.S. Surikova, I.Y. Litovchenko, et al., Acta Mater. 52 (2004) 2067–2074.
[10] W.J. Moberly, J.L. Proft, T.W. Duerig, et al., Acta Metal. Mater. 38 (1990) 2601–2612.
[11] W.J. Moberly, Ultramicroscopy 30 (1989) 395–404.
[12] N.S. Surikova, A.A. Klopotov, E.A. Korznikova, Phys. Metals Metall. 110 (2010) 269–278.